https://doi.org/10.2352/ISSN.2470-1173.2018.10.IMAWM-373

Face Liveness Detection Based on Joint Analysis of RGB and Near-Infrared Image of Faces

Lingxue Song, Changsong Liu; Tsinghua National Laboratory for Information Science and Technology, Department of Electronic Engineering, Tsinghua University; Beijing, China

Abstract

We have witnessed the huge evolution of face recognition technology from the first pioneering works to the current state-of-the-art highly accurate systems in the past few decades. The ability to resist spoofing attacks has not been addressed until recently. While a number of researchers has thrown themselves into the challenging mission of developing effective liveness detection methods against this kind of threat, the existing algorithms are usually affected by limitations such as light conditions, response speed and interactivity. In this paper, a novel and appealing approach is introduced based on the joint analysis of visible image and near-infrared image of faces, three different features (bright pupil, HOG in nose area, reflectance ratio) are extracted to form the final BPNGR feature vector. A SVM classifier with RBF kernel is trained to distinguish between genuine (live) and spoof faces. Experiment results on the self-collected database with 605 samples clearly demonstrate the superiority of our method over previous systems in terms of speed and accuracy.

Introduction

In the field of Mobile Payment and Internet Finance, traditional password is being replaced by biometric authentication techniques, such as face, fingerprint (Touch ID), voice and iris recognition. Liveness detection, which aims at recognition of human physiological activities as the liveness indicator to prevent spoofing attack, is becoming very active in fields of iris recognition and fingerprint recognition. However, the efforts on liveness detection in face recognition are still very limited. On the contrary, it is much easier to acquire a person's face image than it is to acquire other biometric traits like fingerprint or iris. Spoof attacks targeting face recognition systems mainly refers to use a photo, video or 3D mask of an authorized person's face to gain access to services. Experiment shows that state-of-the-art commercial face recognition systems are fragile to attacks of fake faces [1], [2].

The fragility of face recognition systems to face spoof attacks has motivated a number of studies on face liveness detection. Usually, printed or replay attacks that only depending on face images or videos can be easily launched than 3D mask attacks. Therefore, this paper focus on printed and replay attacks and we provide a brief summary and analysis of published face liveness detection methods that targeted for printed or replay spoof attacks as follows.

Motion based methods capture the subconscious motion of facial components or muscles in a live face, such as eye blinking [3], [4], mouth movement [5], [6] and head rotation [7]. These methods require information from multiple frames in order to estimate facial motions. According to [7], the frequency of a facial motion usually ranges from 0.2 to 0.5 Hz. Therefore, we have to spend a relatively long time (> 3s) to collect vitality features for spoofing detection. Additionally, most motion-based methods might be easily fooled by video replay attacks with facial motions.

Texture based methods were proposed to capture the texture difference between genuine face and spoof material (e.g., paper and display screen) resulted from different reflectance properties [8], [9], [10]. Authors in [11] argued that this kind of features (like LBP, HOG, or DoG) are able to recognize artifacts in spoof faces, thus they have achieved great success on some public-domain face spoof databases. However, many texture-based methods have poor generalization ability due to their data-driven characteristic and hence can only work in some particular spoofing scenarios.

Face spoof countermeasures using additional sensors to derive extra information other than 2D intensity face images have also been proposed, such as 3D depth [12], infrared image [13] and voice [14]. These methods show better robustness against limitations like light conditions and pose variations. Although most existing face recognition systems use only RGB cameras, some sensors like IR sensor might be widely embedded in generic cameras in the near future due to its gradually lower cost. For example, the latest iPhone has been equipped with an IR sensor inside its camera.

Liveness detection methods concerning image quality analysis utilize the fact that there will be degradations when recapturing genuine face images or videos in spoof materials, such as color, reflection and blurriness [15], [16], [17]. These degradations almost have nothing to do with facial details, but reflect face image quality differences resulted from different reflection properties of facial components and spoof materials. That is why image distortion analysis based methods usually have better generalization ability, even in the cross-database scenario.

Convolution Neural Network (CNN) has proven to be a powerful tool in many image recognition problems because it is capable of extracting discriminative features directly from the original image data. However, studies on face liveness detection based on deep learning framework are very limited [18], [19], probably owing to the lack of sufficient public available face spoof data, which is usually the guarantee of good performance.

Although a number of face liveness detection methods have been proposed, published studies are subjected to various common factors, such as light conditions, response speed, expensive equipment, high complexity, etc. Hence we aims to develop a simple, fast but effective face liveness detection algorithm that can handle printed attacks (presenting a printed photo to the camera) as well as replay attacks (replaying a previously recorded face video of a target user). The significance of this work in comparison to previous publications is in the following:

1. The first work to use the bright pupil effect of human eyes for face liveness detection.
2. The first work to utilize reflectance information obtained just from RGB and NIR images without particular equipment.
3. Our method requires no user cooperation like blinking eyes or opening mouth, and therefore is user-friendly and fast.
4. Near-infrared light camera is much cheaper and common than Infrared Thermal Camera or 3D camera.

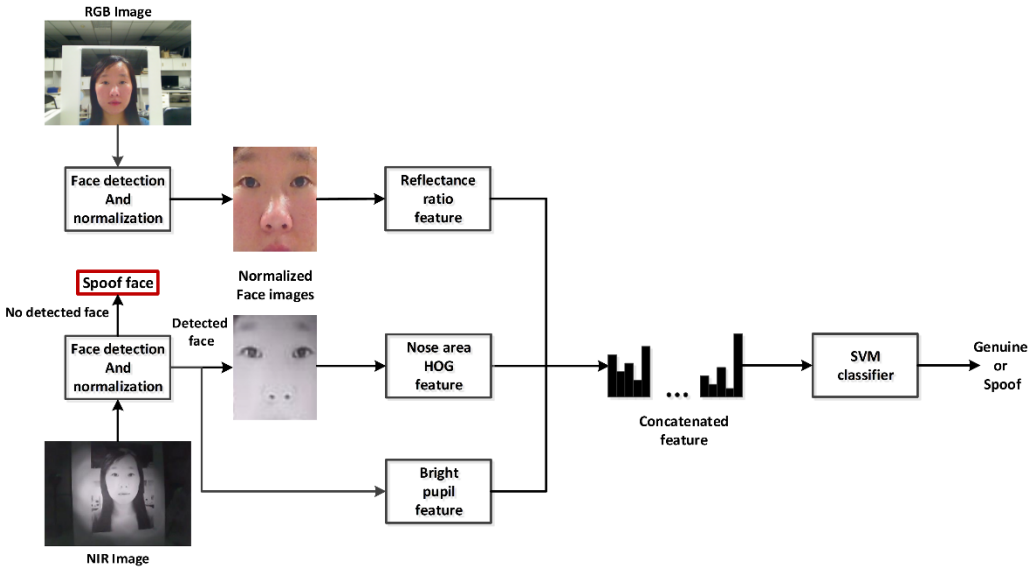

***Figure 1**. The proposed face liveness detection algorithm based on joint analysis of RGB and NIR face images.*

The Proposed Method

Figure 1 shows the system diagram of the proposed algorithm. The input RGB and near-infrared (NIR) face image are first aligned respectively based on two eyes locations and normalized to 81×90 pixels with an interpapillary distance of 49 pixels. For the normalized RGB and NIR face image, three different features are extracted, which are then concatenated into a 23-d feature vector, called BPNGR. This composite feature vector is then fed into a SVM classifier to give the final decision: liveness or spoof face.

Image acquisition

First, we designed an image acquisition system to capture RGB and NIR face images simultaneously. The whole hardware system includes six near infrared light-emitting diodes (LEDs), a RGB camera and a NIR camera that allows the corresponding NIR light (900nm) to pass while cutting off visible light. The six LEDs are tightly distributed evenly on both sides of the NIR camera and coaxial with the camera in order to provide as good as positive light exposure, which, at the same time, guarantees the generation of bright pupil effect of human eyes. A review of our image acquisition system is shown in Figure 2.

***Figure 2**. Overview of image acquisition system.*

During this stage, we investigated the NIR images of various spoof material and found some interesting and useful phenomena : (1) No matter how far the developed photo is from the NIR camera, its NIR image is always totally blank, let alone contains any spoof face. (2) The LEDs inside the LCD screen of common video display devices, such as iPhone, iPad and laptop, do not emit any infrared light. Therefore, their NIR images do not have a clear spoof face, just a fuzzy shadow of a face shape at best. (3) Photos printed with inkjet printer and laser printer can present clear face images under near-infrared light. Sample RGB and corresponding NIR images of spoof faces presented with some spoof material are shown in Figure 3.

Face detection and alignment

Face++ SDK [20] is used for face detection and key-point localization, which works successfully for almost all the faces in our self-collected database. According to the discoveries stated in Image acquisition section, replay attack and developed photo attack can be filtered out in this stage because their NIR images are totally blank. Accordingly, our subsequent algorithm is mainly targeted for printed (Inkjet printing and laser printing) photo attack.

According to [16], face alignment and cropped size will have influences on liveness detection because they decide the degree of contextual information included in feature extraction. We normalized the images to 81×90 pixels with an interpapillary distance of 49 pixels, which contains small contextual information that is helpful in differentiating depth in spoof and genuine faces.

Features extraction

First, we investigate the “bright pupil” effect of genuine face under near-infrared light conditions, which does not exist in printed face’s NIR images. According to that, we extract a 10-d feature vector from a NIR face image by analyzing image pattern in 7×7 cells located in the center of the eyes.

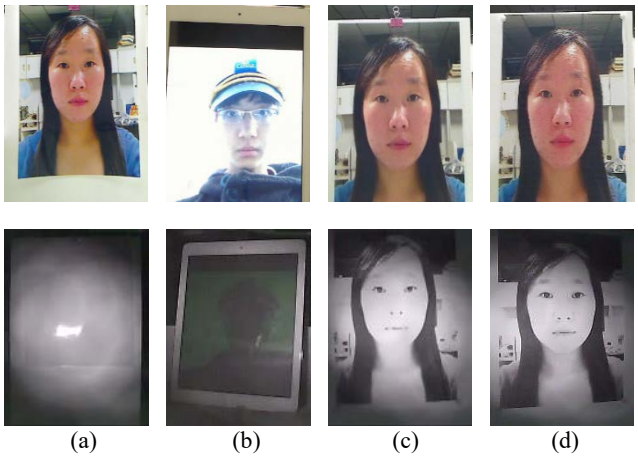

***Figure 3**. Sample RGB and corresponding NIR images of spoof faces presented with some spoof material. (a) developed photo; (b) iPad displayed photo; (c) photo printed by laser printer; (d) photo printed by inkjet printer.*

Second, an obvious difference of genuine and spoof face is observed focus on the texture in nose area of their NIR images, on which a 9-d histogram of oriented gradient feature is extracted.

Finally, we measured the albedo curve of human skin and printed material (Inkjet printing and laser printing), discovered that there are great varieties for printed material at visible wavelengths (400nm~700nm) and near-infrared wavelength (850nm), while the human skin are relatively constant. Therefore, we come up with a method to obtain the reflectance ratio at near-infrared and visible wavelength via joint analysis of RGB and NIR face images, and generate a 4-d feature vector accordingly.

Bright pupil feature

Authors in [21] analyzed the retina reflection under the illumination of different wavelengths. The retina reflects 90% of the incident light at a wavelength of 850nm when it is emitted along the optical axis, while only reflects 40% if replaced with 950nm incident light. In general, in the near-infrared band that ranges from 700nm to 900nm, the human retina can reflect the incident light strongly, which makes the brightness of the human pupil area is much higher than the overall brightness of the entire face in the NIR image. That is exactly what we called the "bright pupil" effect. Some example are shown in Figure 4.

***Figure 4**. Examples of bright pupil effect.*

However, face images with bright pupil effect can only be generated when the light source, the camera and the human eyes are coaxial. Under this circumstance, the retina can completely reflect incident near-infrared light impinging from the front to produce an NIR image with bright pupil effect. Therefore, in our image acquisition system, the near-infrared LEDs are sequentially arranged on the board around the infrared camera, so that the light emitted is approximately parallel to the optical axis of the camera to ensure the generation of the bright pupil effect.

The bright pupil effect of genuine retina does not exist in printed face's NIR images, which provides discrimination between genuine and spoof face. Figure 5 abstracted the characteristics of genuine and spoof face's eye area in their NIR images. In addition to the fact that the intensity of genuine pupil area is much higher than the intensity of spoof pupil area, the eye area pattern of genuine face is roughly bright in the middle (pupil area), dark around (the white of the eye), while the spoof face is the opposite.

***Figure 5**. NIR image characteristics of the eyes area. (a) genuine eyes; (b) printed spoof eyes.*

According to the findings mentioned above, we designed a method to extract bright pupil feature: Firstly, the coordinates of both eyes are detected in the input near-infrared image, and pixel blocks of 7×7 px size are taken centering on the left and right eye coordinates respectively. Then we take four circles outward starting from the center of the left eye's pixel block and calculate the average gray value of all the pixels in each circle as the first 4-dimensional features of the left eye's feature vector. Finally, the ratio of the average grayscale value of the pixel block to the average grayscale value of the normalized face near-infrared image is calculated as the fifth dimension of the left eye's feature vector. The same feature extraction operation is done for the right eye. Feature vectors of both eyes are cascaded to form a 10-dimensional vector as the final bright pupil feature of the input near-infrared image.

Nose area HOG feature

Observing the NIR images of genuine and spoof faces shown in Figure 4 and Figure 3, the differences between them can be intuitively perceived, especially in facial components area, which should be captured if we use traditional texture features (like LBP, HOG, or DoG) directly on the whole face. However, to avoid complex computation and reusing the information of the eyes, we intend to focus only on some most discriminating facial areas.

Figure 6 shows the comparison in the nose area of genuine and spoof near-infrared face images. It can be obviously noticed that there are clear differences in texture between genuine and spoof sample. The shape and edges of genuine nose including lacrimal groove are clearly visible. However, these texture clues have greatly reduced in the spoof sample, or even disappeared. For this reason, we decide to extract texture features only from the nose area.

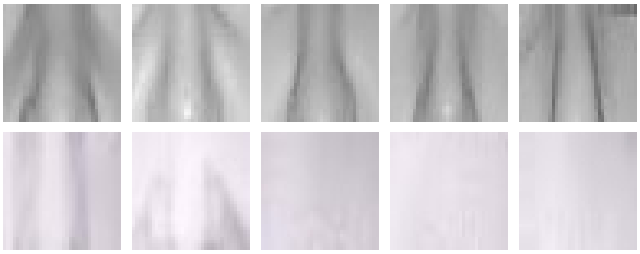

***Figure 6**. The comparison in the nose area of genuine (first row) and spoof (second row) near-infrared face images.*

Histogram of Oriented Gradient (HOG) feature was first proposed by Dalal at CVPR 2005 and they achieved good results in pedestrian detection. In practice, the author first divides an image window into some small spatial areas (called cells). For each cell, the gradient direction of each pixel in the cell is accumulated as a local histogram. In order to cope with light changes, shading and other factors, the author accumulates a measure of the local histograms in a slightly larger area (called block), and then uses this cumulative result to normalize all the cells in the block. This normalized block description operator is called the Histogram of Oriented Gradient descriptor by the author.

In our case, the NIR image will not be affected by uncontrolled ambient light conditions and our target nose area is small enough to avoid problems arises from the difference in foreground and background contrast. Therefore, we simplified the original HOG feature extraction procedure accordingly. Specifically, we treated the whole target nose area (normalized into 32×32 px grayscale image) as a "cell" and calculated its HOG descriptor as the final feature vector directly without the block normalization procedure. We set the bin number of the histogram as nine, so our final nose area HOG feature is a 9-dimensional vector.

Reflectance ratio feature

Reflectance analysis

According to the Lambertian reflectance model [22], the reflectance light intensity at location (x, y) is:

$$I(x,y) = A_0(x,y)r(x,y)cos\theta(x,y) \quad (1)$$

in which $r(x,y)$ is the material albedo, $A_0(x,y)$ is the incident light intensity and $\theta(x,y)$ is the angle between the surface normal vector and the reflected light receiver's viewpoint.

For the purpose of differentiating genuine and spoof faces, the albedo should be the most discriminating information. We measured the albedo curves of genuine skin and some common spoof materials, which include developed photo paper and two kinds of printed photo papers. The curves is shown in Figure 7. As can be seen from the curves, the albedo of genuine skin is quite low and relatively constant in both visible and near-infrared bands. In contrast, no matter what spoof material it is, its albedo is always much higher than skin's in the whole band and its albedo is relatively low in visible band while quite high in near-infrared band.

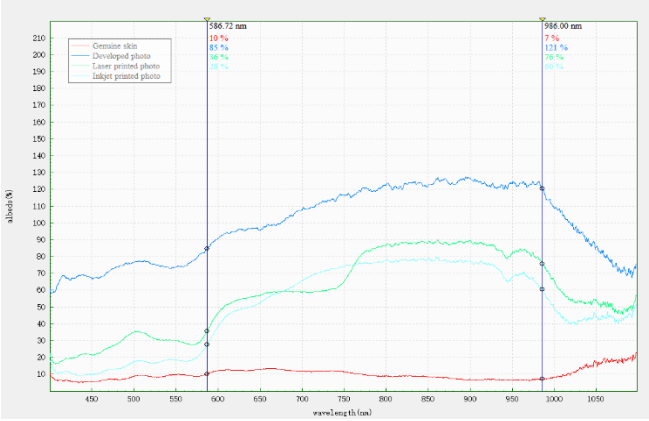

***Figure 7**. The albedo curves of skin and spoof materials.*

Reflectance ratio estimation

According to the above analysis, if we can obtain the material's albedo, it will be quite easy to distinguish genuine and spoof faces. However, albedo is not an easily measurable characteristic, which usually depends on some special instruments like spectrometers. Therefore, we try to estimate albedo related information from just RGB and NIR images without extra equipment.

For the image location (x, y), under near-infrared light, equation (1) can be written as:

$$I_{NIR}(x,y) = A_{NIR}(x,y)r_{NIR}(x,y)cos\theta(x,y) \quad (2)$$

Visible light contains a range of wavelength with different albedo. Here we assumed that there is a mean albedo, expressed as r_{VIS}. In this way, for the same image location under visible light, equation (1) can be expressed as:

$$I_{VIS}(x,y) = A_{VIS}(x,y)r_{VIS}(x,y)cos\theta(x,y) \quad (3)$$

In equation (2) and (3), we assumed that $\theta(x,y)$ is the same. Then the ratio of the two intensity values is:

$$\frac{I_{NIR}(x,y)}{I_{VIS}(x,y)} = \frac{A_{NIR}(x,y)r_{NIR}(x,y)}{A_{VIS}(x,y)r_{VIS}(x,y)} \quad (4)$$

The above intensity ratio does not purely contain the albedo ratio (also reflectance ratio) that we are interested in, but also the incident light that we would like to remove. Suppose that there exists a point or an area in all face images, which is white under both visible and near-infrared light, that is $r_{NIR} = r_{VIS} = 1$, then for this point or area, equation (4) becomes:

$$\frac{I_{NIR}(x,y)}{I_{VIS}(x,y)} = \frac{A_{NIR}(x,y)}{A_{VIS}(x,y)} = \frac{1}{k} \quad (5)$$

in which we use k to stand for this special intensity ratio and call it *correction factor*. If we multiply equation (4) with this correction factor, we can get:

$$k * \frac{I_{NIR}(x,y)}{I_{VIS}(x,y)} = k * \frac{A_{NIR}(x,y)r_{NIR}(x,y)}{A_{VIS}(x,y)r_{VIS}(x,y)} = \frac{r_{NIR}(x,y)}{r_{VIS}(x,y)} \quad (6)$$

As a result, only the reflectance ratio information is left in the image intensity ratio, eliminating the influence of incident light. In practice, we can slightly relax this constraint of absolute whiteness area by approximating it with white walls which need to be very close to the face to ensure the consistent light intensity.

Reflectance ratio feature extraction

Based on the analysis above, we designed a procedure to extract reflectance ratio related features: Firstly, we extract 16×16 px block from the wall area of input RGB and NIR face images respectively and calculate the ratio of the average gray values of RGB and NIR pixel block as the correction factor under this light condition. Then we choose four blocks from cheek area of the RGB and NIR faces respectively. Using cheek area is to ensure that the albedo is stable in this area and the $\theta(x,y)$ can be considered approximately the same. For each block, we calculate the ratio of the average gray values of NIR and RGB image and multiply it with the correction factor as the block's reflectivity feature. Finally, the features of four blocks are cascades to form the reflectance ratio feature vector of dimension 4.

The above three types of feature (bright pupil, HOG in nose area and reflectance ratio) are finally concatenated into a BPNGR feature vector with 23 dimensions.

Classification with Support Vector Machines

As one of the best and most commonly used classifiers, the Support Vector Machine (SVM) [23] is often applied to various classification and regression problems. It describes the data distribution in a structured way, reducing the size and distribution requirements of the data, giving it excellent generalization ability. SVM can get much better results than other algorithms when the training set is small, so we choose SVM as the two-class classifier.

Experimental Results and Discussion

To evaluate the effectiveness of face liveness detection algorithms, a few published papers have made their face spoof database publicly available as benchmarks, such as CASIA-FASD [24], NUAA [25] and Idiap REPLAY-ATTACK database [26]. However, none of the publicly available databases contains both visible and near-infrared images of spoof faces at the same time. Therefore, we built a new database to test our liveness detection algorithm.

Dataset Collection

In our experiment, a positive sample refers to the RGB and corresponding NIR image pair of a genuine face, a negative sample refers to the RGB and corresponding NIR image pair of a spoof face. The RGB images with 1600×1200 px are photographed using Canon EOS 10D digital camera and the NIR images with 320×240 px are collected using 850nm near-infrared camera.

A total of 128 individuals are included in our dataset, one positive sample for each subject. Then we print their high-resolution RGB images on A4 papers using laser printer and inkjet printer as our spoof samples. For 31 of the total subjects, we collect face images (RGB and NIR) of laser-printed photo and inkjet-printed photo at three distance of 40cm, 50cm and 60cm respectively, making 186 (31×3×2) negative samples. For the remaining 97 subjects, only images of laser-printed photo are collected at that three distances respectively, making 291 (97×3×1) negative samples. As a result, we built a dataset with 128 positive samples and 477 negative samples, totally 1210 images were taken.

Results and Discussion

We perform our experiments on a computer with 16GB of memory and one Intel processor with i7-6700U cores at 3.40 GHz. A SVM with RBF kernel implemented by libSVM is applied as the classifier. We use 424 samples to train a SVM classifier and test it on the remaining 181 samples. Five-fold cross validation is implemented to do the parameter selection of the penalty coefficient and kernel radius. Our method was able to achieve almost perfect liveness detection task, yielding total classification accuracy of 99.4%, false acceptance rate of 0.7% and false rejection rate of 0%.

Because that our dataset is not public, it is impossible to directly compare with other state-of-the-art algorithms. Most of these algorithms are not open-source and therefore must be re-implemented in our dataset. For comparison, we re-implemented a state-of-the-art algorithm based on the LBP features [9], which achieved total classification accuracy of 98% on the NUAA database, and evaluated it on our spoof dataset. The original algorithm in the literature is to extract several local and global LBP features to form an 833-dimensional feature vector. However, the authors of [26] pointed out that increasing the dimensionality of the LBP feature vector does not help improve performance. Since the global LBP feature vector is computationally more efficient, we modify the algorithm of [9] slightly in the re-implementation and extract several channels global LBP features to form a 479-dimensional feature vector. Table 1 compares the LBP-based method and the proposed method on our spoof dataset.

Table 1: Performance comparison between our proposed approach and the state-of-the-art LBP based method on our spoof dataset

Method	AUC	TPR@ FAR=0.1	TPR@ FAR=0.01
LBP-based	0.96	96.5%	39.4%
Our approach	0.99	99.3%	99.3%

As can be seen from Table 1, our algorithm achieves better classification performance. In addition to that, our BPNGR feature vector is only 23 dimensions, which is much lower than the state-of-the-art LBP based method. Further, the average time for extracting an image's BPNGR feature is only 0.009 seconds, while the comparative algorithm takes 0.387 seconds to extract 479-dimensional LBP feature vectors.

Conclusions

In this paper, we proposed an efficient and effective method for face liveness detection by joint analysis of RGB and NIR images of faces. Three types of features (bright pupil, HOG in nose area, reflectance ratio) have been designed to capture the discriminative differences between genuine and spoof faces, which are concatenated together, resulting in a 23-dimensional BPNGR feature vector. A SVM classifier is used to distinguish between genuine and spoof faces. We have also collected a face spoof dataset that contains spoof face images captured with NIR camera. Evaluations on this self-collected dataset demonstrate that our approach performs better than LBP based algorithm in terms of both accuracy and speed. Furthermore, our method requires only cheap NIR sensors that have been widely used in surveillance cameras and cellphones, which is much more practical than methods relying on thermal or 3D cameras.

Our plans for future work on face liveness detection include: 1) enlarge our face spoof dataset into a representative database containing more spoof attack types like high quality 3D mask attacks and more scenarios; 2) develop ways to further improve the robustness of our BPNGR features in challenging situations, for example, find a better way to calculate correction factor when there is no white wall in the background.

Acknowledgment

This work was supported by the National Basic Research Program of China (973 program) under Grant No. 2013CB329403 and the National Natural Science Foundation of China under Grant No. 61471214.

References

[1] D. Wen, H. Han and A. K. Jain, "Face Spoof Detection With Image Distortion Analysis," in IEEE Transactions on Information Forensics and Security, vol. 10, no. 4, pp. 746-761, April 2015.

[2] A. Anjos and S. Marcel, "Counter-measures to photo attacks in face recognition: A public database and a baseline," 2011 International Joint Conference on Biometrics (IJCB), Washington, DC, 2011.

[3] G. Pan, L. Sun, Z. Wu and S. Lao, "Eyeblink-based Anti-Spoofing in Face Recognition from a Generic Webcamera," 2007 IEEE 11th International Conference on Computer Vision, Rio de Janeiro, pp. 1-8 , 2007.

[4] L. Sun, G. Pan, Z. Wu, and S. Lao, "Blinking-based live face detection using conditional random fields," in Proc. AIB, pp. 252–260, 2007.

[5] K. Kollreider, H. Fronthaler, M. I. Faraj and J. Bigun, "Real-Time Face Detection and Motion Analysis With Application in "Liveness" Assessment," in IEEE Transactions on Information Forensics and Security, vol. 2, no. 3, pp. 548-558, Sept. 2007.

[6] A. K. Singh, P. Joshi and G. C. Nandi, "Face recognition with liveness detection using eye and mouth movement," 2014 International Conference on Signal Propagation and Computer Technology (ICSPCT 2014), Ajmer, pp. 592-597, 2014.

[7] S. Bharadwaj, T. I. Dhamecha, M. Vatsa and R. Singh, "Computationally Efficient Face Spoofing Detection with Motion Magnification," 2013 IEEE Conference on Computer Vision and Pattern Recognition Workshops, Portland, OR, pp. 105-110, 2013.

[8] I. Chingovska, A. Anjos and S. Marcel, "On the effectiveness of local binary patterns in face anti-spoofing," 2012 BIOSIG - Proceedings of the International Conference of Biometrics Special Interest Group (BIOSIG), Darmstadt, pp. 1-7, 2012.

[9] J. Määttä, A. Hadid and M. Pietikäinen, "Face spoofing detection from single images using micro-texture analysis," 2011 International Joint Conference on Biometrics (IJCB), Washington, DC, pp. 1-7, 2011.

[10] W. Kim, S. Suh and J. J. Han, "Face Liveness Detection From a Single Image via Diffusion Speed Model," in IEEE Transactions on Image Processing, vol. 24, no. 8, pp. 2456-2465, Aug. 2015.

[11] J. Yang, Z. Lei, S. Liao and S. Z. Li, "Face liveness detection with component dependent descriptor," 2013 International Conference on Biometrics (ICB), Madrid, pp. 1-6, 2013.

[12] N. Erdogmus and S. Marcel, "Spoofing in 2D face recognition with 3D masks and anti-spoofing with Kinect," 2013 IEEE Sixth International Conference on Biometrics: Theory, Applications and Systems (BTAS), Arlington, VA, pp. 1-6, 2013.

[13] Z. Zhang, D. Yi, Z. Lei and S. Z. Li, "Face liveness detection by learning multispectral reflectance distributions," Face and Gesture 2011, Santa Barbara, CA, pp. 436-441, 2011.

[14] G. Chetty, "Biometric liveness checking using multimodal fuzzy fusion," International Conference on Fuzzy Systems, Barcelona, pp. 1-8, 2010.

[15] J. Galbally, S. Marcel and J. Fierrez, "Image Quality Assessment for Fake Biometric Detection: Application to Iris, Fingerprint, and Face Recognition," in IEEE Transactions on Image Processing, vol. 23, no. 2, pp. 710-724, Feb. 2014.

[16] D. Wen, H. Han and A. K. Jain, "Face Spoof Detection With Image Distortion Analysis," in IEEE Transactions on Information Forensics and Security, vol. 10, no. 4, pp. 746-761, April 2015.

[17] D. C. Garcia and R. L. de Queiroz, "Face-Spoofing 2D-Detection Based on Moiré-Pattern Analysis," in IEEE Transactions on Information Forensics and Security, vol. 10, no. 4, pp. 778-786, April 2015.

[18] D. Menotti et al., "Deep Representations for Iris, Face, and Fingerprint Spoofing Detection," in IEEE Transactions on Information Forensics and Security, vol. 10, no. 4, pp. 864-879, April 2015.

[19] Alotaibi A and Mahmood A, " Deep face liveness detection based on nonlinear diffusion using convolution neural network," Signal, Image and Video Processing, vol. 11, no. 4, pp. 713-720, May 2017.

[20] Face++ SDK, Available: https://www.faceplusplus.com.cn/face-landmark-sdk/

[21] Morimoto C H, Koons D and Amir A, "Pupil Detection and Tracking Using Multiple Light Sources," Image and Vision Computing, vol. 18, no. 4, pp. 331-335, March 2000.

[22] R. Basri and D. W. Jacobs, "Lambertian reflectance and linear subspaces," in IEEE Transactions on Pattern Analysis and Machine Intelligence, vol. 25, no. 2, pp. 218-233, Feb 2003.

[23] C.-C. Chang and C.-J. Lin, " LIBSVM: a library for support vector machines," ACM Transactions on Intelligent Systems and Technology, vol. 2, no. 3, pp. 27:1–27:27, May 2011.

[24] Z. Zhang, J. Yan, S. Liu, Z. Lei, D. Yi and S. Z. Li, "A face antispoofing database with diverse attacks," 2012 5th IAPR International Conference on Biometrics (ICB), New Delhi, pp. 26-31, 2012.

[25] X. Tan, Y. Li, J. Liu, and L. Jiang, "Face liveness detection from a single image with sparse low rank bilinear discriminative model," in Proc. ECCV, pp. 504–517, Sep. 2010.

[26] I. Chingovska, A. Anjos and S. Marcel, "On the effectiveness of local binary patterns in face anti-spoofing," 2012 BIOSIG - Proceedings of the International Conference of Biometrics Special Interest Group (BIOSIG), Darmstadt, pp. 1-7, 2012.

Author Biography

Lingxue Song received her BE in Telecommunications Engineering from Tianjin University of China (2015) and she is currently a 3th-year Ph.D. student from Department of Electronic Engineering, Tsinghua University, China. Her research interests lie in computer vision and pattern recognition, with particular interest in face recognition related issues.